

# **PHY499: Undergraduate Thesis**

Statistical Analysis of Noise in Field Effect  
Transistors



**Ritwik Bandyopadhyay**

Supervisors:

Dr. Samarendra Pratap Singh

Dr. Santosh Kumar

Department of Physics  
Shiv Nadar University

# **Declaration**

I declare that this thesis has been composed solely by myself and that it has not been submitted, in whole or in part, in any previous application for a degree. Except where stated otherwise by reference or acknowledgment, the work presented is entirely my own.

Ritwik Bandyopadhyay

Dr. Samarendra Pratap Singh

Dr. Santosh Kumar

# **Abstract**

Stochastic Resonance has received growing interest as a method of improving device performance by using external noise. Ionic liquids have emerged as materials that give very high capacitance values when used as gate dielectrics, leading to large charge carrier concentrations in the conduction channel. In this project, we aim to demonstrate improvement in signal detection performance of an ionic liquid gated organic field effect transistor by the use of stochastic resonance. For this purpose, an ionic liquid gated organic field effect transistor was fabricated. Then, square voltage signals of different frequencies were used as input signals and the ability of the device to detect the signals was enhanced using stochastic resonance.

# Acknowledgements

I would like to thank my family for always supporting me and being a source of love and warmth. I would also like to thank my friends in Ahmedabad and in SNU for the joy they bring to my life. Dr. Samarendra Pratap Singh and Dr. Santosh Kumar, the supervisors for this project have inspired me throughout the course of this project and have been a source of wisdom. Lastly I would like to thank Yogesh Yadav, Bishwajit Mandal and Ushasri Mukherjee for helping in the fabrication process and for teaching me the laboratory techniques needed to carry out this project.

# Dedication

Dedicated to Messi Bandyopadhyay, without whose company, online lectures would have been impossible to attend.



Figure 1: Messi Bandyopadhyay

# Contents

<b>1</b>	<b>Introduction</b>	<b>7</b>
1.1	Context of Research . . . . .	7
1.2	Problem of Interest . . . . .	8
1.3	Limitations . . . . .	9
<b>2</b>	<b>Review of Literature</b>	<b>10</b>
2.1	Stochastic Resonance . . . . .	10
2.2	Ionic Liquids and Electrolyte Gating . . . . .	12
2.2.1	Electric Double Layer . . . . .	13
<b>3</b>	<b>Procedures and Methodologies</b>	<b>15</b>
3.1	Device Fabrication . . . . .	15
3.1.1	Materials . . . . .	15
3.1.2	Device Structure . . . . .	16
3.1.3	Fabrication Process . . . . .	17
3.2	Experimental Setup for SR . . . . .	17
<b>4</b>	<b>Results and Findings</b>	<b>18</b>
4.1	Device Characterisation . . . . .	18
4.2	Stochastic Resonance . . . . .	20
4.3	Frequency 750mHz . . . . .	21
4.4	Frequency 500mHz . . . . .	23
4.5	Frequency 250mHz . . . . .	24
<b>5</b>	<b>Conclusions</b>	<b>27</b>
5.1	Conclusions . . . . .	27
5.2	Scope for future work . . . . .	27

# Chapter 1

## Introduction

### 1.1 Context of Research

The advent of the electronics revolution has been driven by the replacement of bulky, expensive, difficult to manufacture and fragile vacuum devices by their solid state semiconductor counterparts. It is widely accepted that the beginning of this revolution was the invention of the transistor at bell labs in 1947. Today, there are trillions of transistors in use in devices around the world[1] and they are the basic building block for most electronic devices.

Rapid advancement in semiconductor device technology was observed in the following years with the invention of the integrated circuit in the 1960s. Integrated circuits allowed for multiple circuits, including their different components to be made out of the same piece of semiconductor material. This led to Gordon Moore (one of the co founders of Intel) making the claim that came to be known as Moore's law. Moore's law claimed that the number of components in an integrated circuit would double every two years. This held true for a long time until finally physical quantum mechanical limitations were reached in the beginning of the 21st century.

The 21st century has posed its own set of challenges. Most recently, there has been a global chip shortage due to complex geopolitical reasons. In order to understand this, it is important to note that most of the advanced semiconductor chips used today are manufactured in a few select Asian countries (with the exception of The United States of America). Taiwan and China together account for almost 60% [2] of the semiconductor chip supply. Hence, when the Covid-19 pandemic struck and there were trade bans imposed by the United States on China, large disruptions were caused in supply chains leading to global shortages of high quality semiconductor chips. It is important to note that, most of these chips are Silicon wafer based which require highly specialised machinery to manufacture. Complex processes are

also required to mine Silicon from the Earth and most of the world's Silicon deposits are concentrated in China[3], lending to further localisation of production and potential supply chain issues.

The factors outlined above have made developments in non-silicon based semiconductor technology of great interest. Semiconducting Organic Polymer based technology has shown great potential as replacement for silicon based devices. Organic polymers are easier to synthesize as compared to the intensive mining and refining processes that are undertaken to obtain high quality silicon. Since the 2010s, Organic Light Emitting Diode (OLED) based displays have been utilised in many commercial products ranging from Televisions to Mobile Phones.

An emerging area of interest in organic electronic devices has been the utilisation of stochastic resonance. Stochastic resonance is a phenomenon that assists in a system's ability to detect weak periodic signals[4]. It has been demonstrated in purely organic systems such as crayfish[5] and in organic electronic devices. In many applications of transistors, the environment in which they are positioned consist of background noise. The ability to not only make the device resistant to the negative effects of background noise but to utilise it to enhance device performance would be of great use and hence it has captured the interest of researchers.

## 1.2 Problem of Interest

One category of organic semiconductor based devices being widely researched today is Organic Field Effect Transistors (OFETs). OFETs are devices in which, the semiconducting layer of the Field Effect Transistor is replaced by an organic semiconductor. These devices can be used in the development of sensors and have shown light emitting characteristics [6].

Organic semiconductor based sensors have potential use cases in a variety of industries. Low power consumption is a desirable property for these sensors. Ionic liquid gating has emerged as a method for achieving high charge carrier densities in the conduction channel through electric-double layer formation, leading to lower energy costs in device operation. [7]. In this project, we demonstrate a phenomenon that potentially reduces the power consumption of an Ionic Liquid gated Organic Field Effect Transistor (IL-OFET) when sensing an electrical signal. An IL-OFET was fabricated and electrical characterisation was carried out. Then, Square wave signals were used as input signals at the Gate terminal of the IL-OFET. This was performed at different Gate offset biases (in the On and Sub-Threshold regions). The phenomenon of Stochastic Resonance (SR) was exploited to detect the signal

at lower Gate biases, leading to lower power consumption.

### 1.3 Limitations

Ionic liquid gated organic field effect transistors are slow devices. This means they respond poorly to high frequency switching. As a result, the frequencies used in this project were in the mHz range. Many practical applications would require the ability to work with higher frequencies and hence developing faster IL-OFETs would be desirable. Also, compound signals consisting of multiple frequencies were not used since the process of stochastic resonance relies on using noise to amplify the signal. More than one frequency present in the input signal would lead to distortion in the output compared to the input signal, which would make it harder to assess detection performance.

# Chapter 2

## Review of Literature

### 2.1 Stochastic Resonance

Stochastic resonance (SR) is a phenomenon wherein the superposition of noise on a weak signal can help amplify it. This allows sensing devices to detect weak signals that would otherwise go undetected (See fig2.1). Three conditions must be satisfied in order to observe SR.

- A thresholding device.
- A weak periodic signal.
- A source of noise.

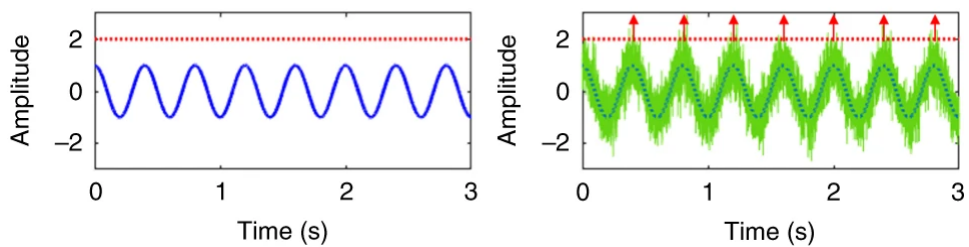


Figure 2.1: A Schematic representing SR [8]

SR has been demonstrated in a variety of systems, even mechanoreceptors on a crayfish tailfan[5] . The mechanoreceptors consist of hair on the tailfan, that in response to motion cause spikes in associated sensory neurons. The power spectral density was observed in response to signals in the absence and presence of noise of varying intensities. It was found that the performance of these mechanoreceptors increased in the presence of an intermediate amount of noise and decreased at high

noise values. SR has also been demonstrated in man-made systems like in Poly(3-hexylthiophene-2,5-diyl (P3HT) based Organic Field Effect Transistors (OFETs)[4]. The threshold gate voltage can act as the thresholding device with constant drain source potentials. Correlation coefficient defined between the input and output signals can be used as a measure of the signal transmission performance.

Researchers have demonstrated SR in inorganic MoS<sub>2</sub> based field effect transistors[8]. The study included two demonstrations of SR, one in MoS<sub>2</sub> based FET and one in MoS<sub>2</sub> based photodetectors. We will highlight the setup and the methodology used for the demonstration in the MoS<sub>2</sub> FET. Once fabricated, the transistor potential across the Drain and Source ( $V_{DS}$ ) electrodes was held at a constant level. A square wave of 2.5 Hz was applied at the Gate potential ( $V_{GS}$ ) and the resulting current across the Drain and Source electrodes ( $I_{DS}$ ) was measured. The square wave was applied with different offset biases, so as to measure the response in the ‘On’, ‘Subthreshold’ and ‘Off’ state of the FET. The  $I_{DS}$  was sampled at 20Hz and instead of defining correlation coefficients, a Fourier transform was performed on the  $I_{DS}$  time series data and its absolute value was studied to formulate a power spectral density (PSD) plot. It was observed that the signal was detected in the On state, however, no coherent signal was detected in the Off and Subthreshold state (See fig2.2). Next, Gaussian noise of varying standard deviation was superimposed on the square wave signal and was applied across the  $V_{GS}$  and the current response in  $I_{DS}$  was measured. Once again, a Fourier transform was carried out of the time series  $I_{DS}$  data and it was found that for certain values of standard deviation, the signal that previously went undetected in the Off and Subthreshold states, was now detected in the form of spikes in the PSD plots (See fig2.3).

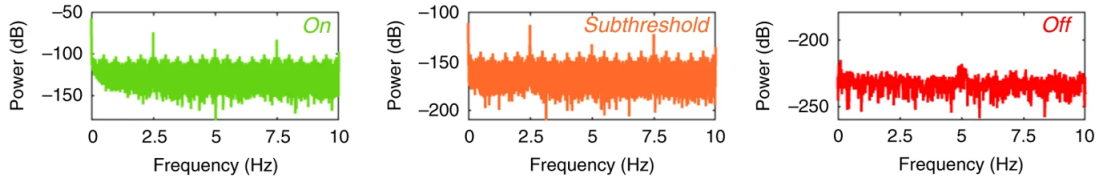


Figure 2.2: The PSD plots in response to the signal without noise superimposed on it.[8]

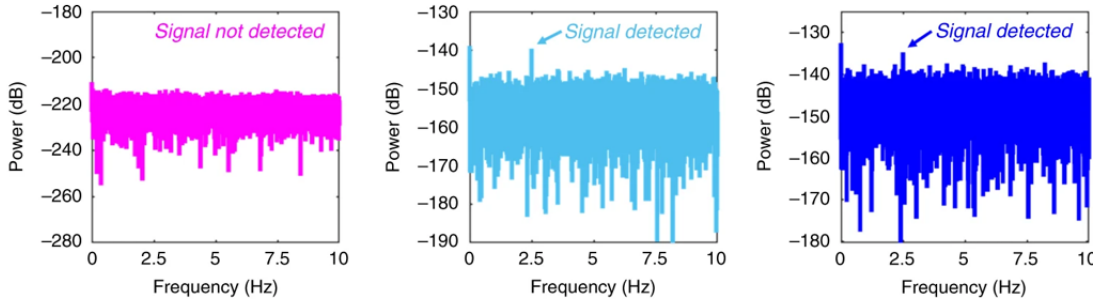


Figure 2.3: The PSD plots in response to the signal with noise superimposed on it for varying values of standard deviation.[8]

## 2.2 Ionic Liquids and Electrolyte Gating

The Gate terminal plays a key role in the operation of FETs. As larger magnitudes of gate potential are applied, more charge carriers are induced in the conduction channel, causing larger current to flow through the channel. However, it is essential to put a layer of insulating material (usually referred to as the ‘gate dielectric’) between the gate electrode and the conduction channel, to prevent the current from ‘leaking’ through the gate electrode. It has been common practice to use oxides such as Silicon Dioxide and Aluminium Oxide as the gate dielectric. The gate electrode along with the dielectric and the semiconducting layer form what is referred to as a MOS (Metal Oxide Semiconductor) capacitor [9]. In this capacitor, the gate electrode and the semiconducting layer with free charge carriers form the plates and the insulating material in between acts as the capacitor dielectric (See fig2.4).

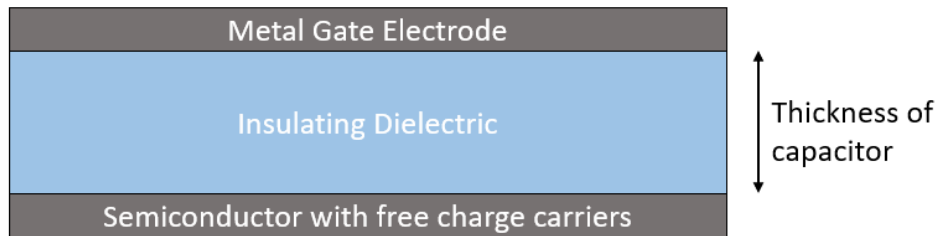


Figure 2.4: Schematic for a MOS capacitor

While the conventional dielectric materials are solid state, there have been recent reports of devices utilising liquid electrolytes as the gate dielectric [7]. In this project, we are specifically concerned with a class of electrolytes referred to as Ionic Liquids. Ionic Liquids refer to organic salts that remain in the liquid state at 100°C and below.

### 2.2.1 Electric Double Layer

A phenomenon known as electric double layer formation, that occurs when an electrolyte comes in contact with a charged electrode, is utilised in such devices to give very high capacitance values, leading to high charge carrier densities in the conducting channel. An electric double layer (EDL) forms at the interface between a charged surface and a liquid electrolyte. The charges at the surface of the electrode, strongly attract the mobile charges in the electrolyte, leading to a thin layer of oppositely charged ions placed right next to each other (See fig2.5).

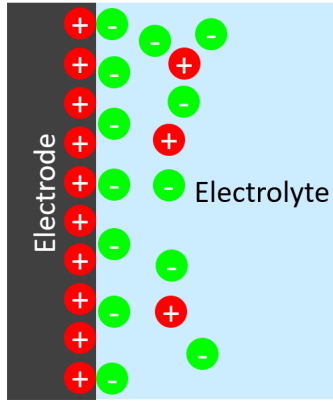


Figure 2.5: Schematic explaining Electric Double Layer formation

These EDLs can be modeled as parallel plate capacitors with very small distances between the parallel plates. We know the capacitance of a parallel plate capacitor is given by,

$$C = \frac{\epsilon A}{D} \quad (2.1)$$

where  $A$  is the cross sectional area of the plates,  $\epsilon$  is the permittivity of the capacitor dielectric and  $D$  is the separation between the plates of the dielectric. In the case of these EDLs, the distance  $D \simeq$  few ion diameters, leading to very high values of capacitance. Such electric double layers are formed at both contact surfaces and hence the total capacitance can be modeled as a series combination of two such capacitors [10]. Note that the capacitance of each is different since one surface is a metal-electrolyte interface whereas the other one is a semiconductor-electrolyte interface.

When a potential is applied across an electrode and a semiconductor, most of the potential drops across the liquid solid interfaces. The thickness of the layer of accumulated ions is largely independent of the thickness of the electrolyte dropped. This is very different from the behaviour of solid state insulator materials[7]. The potential drops almost linearly across the material and hence the charge accumula-

tion depends heavily on the thickness of the layer of insulator deposited (See fig2.6).

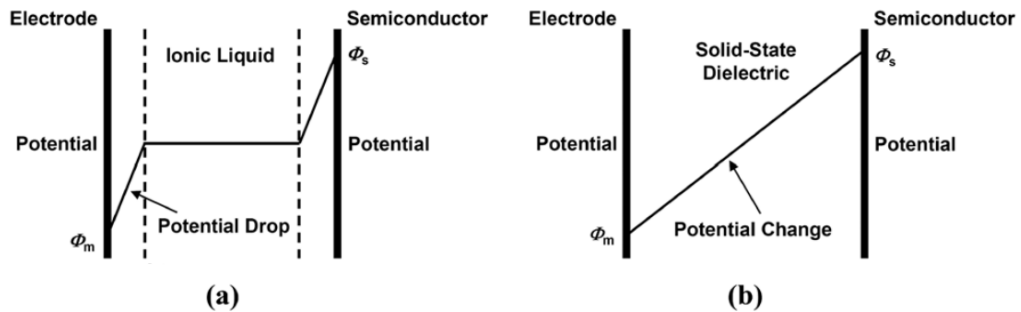


Figure 2.6: Potential changes in the dielectric materials, sandwiched by an electrode and a semiconductor, for ionic liquids (a) and solid-state dielectrics (b).[7]

# Chapter 3

## Procedures and Methodologies

### 3.1 Device Fabrication

This section describes in detail the materials used for fabricating the device, the structure of the device and the methodologies used to fabricate the device.

#### 3.1.1 Materials

The substrate used to make the device is Indium Tin Oxide (ITO) coated glass. The ITO coated glass substrates are pre-patterned with source drain contacts (See fig3.1). ITO is a widely used conducting transparent oxide. Its transparency and conductance make it an ideal candidate for photovoltaic devices. The ITO coated glass substrates were sourced from Ossila [11].



Figure 3.1: ITO coated glass [11]

Poly(3-hexylthiophene-2,5-diyl) (See fig3.2) or P3HT is a low band gap organic polymer donor and was used as the semiconducting layer. It has been popularly used as the semiconducting layer for thin film organic field effect transistors and

organic photovoltaic devices due to its thermal stability, semiconducting properties and commercial availability[12]. Highly regioregular P3HT (MW 30 900 and regioregularity 99%) was purchased from TCI chemicals. Using Chlorobenzene as the solvent instead of the usual Chloroform has shown higher performance in P3HT organic field effect transistors (OFET) devices [13]. Hence, Chlorobenzene was used as the solvent.

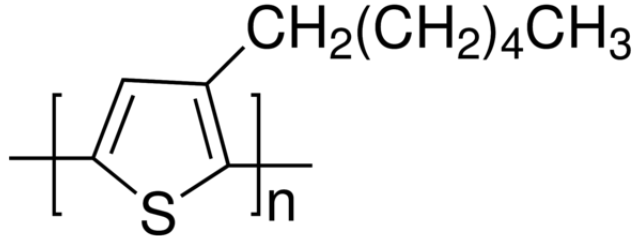


Figure 3.2: Structure of P3HT [14]

A study was conducted on the performance of various Ionic Liquids as gate dielectrics in P3HT based IL-OFETs [13], using the same ITO coated substrate. In the study, 1-ethyl-3-methylimidazolium tetrafluoroborate (See fig3.3)(EMIM BF<sub>4</sub>) was found to have the best performance. Hence, it was used as the gate dielectric in the device fabricated for this study.

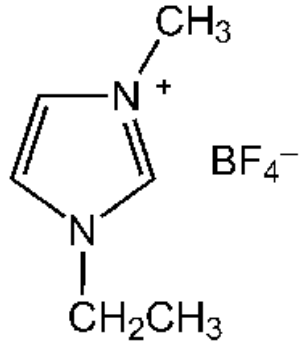


Figure 3.3: Structure of EMIM BF<sub>4</sub>[15]

### 3.1.2 Device Structure

The IL-OFET was fabricated with a bottom contact top gated design. The substrate layer used was glass with a pre-patterned ITO coating. The ITO layer acted as the drain and source electrodes. A thin film of P3HT acted as the semiconducting layer, on top of which, a drop of EMIM BF<sub>4</sub> Ionic Liquid acted as the gate dielectric. A floating platinum electrode was used as the gate electrode (See fig3.4).

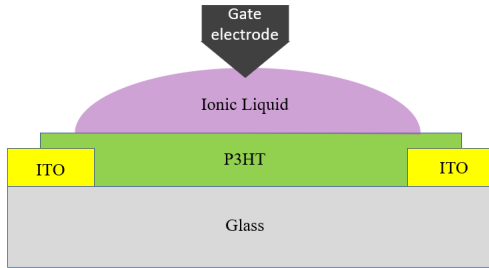


Figure 3.4: Device Schematic

### 3.1.3 Fabrication Process

Glass substrate with pre-patterned ITO coating was purchased from Ossila. The substrate was cleaned using Ultrasonication and then was treated with UV Ozone at 100°C for 20 minutes. P3HT was purchased from TCI Chemicals and Chlorobenzene was used as the solvent. The solution was prepared by using 1mg/ml of P3HT in Chlorobenzene in a vial. The vial was then kept at 60°C in a magnetic stirrer for 15 hours. Once the solution was prepared, it was spin coated onto the ITO coated glass substrate at 1000RPM for 1 minute. Post spin coating, the solvent was allowed to evaporate for 24 hours. Before carrying out electrical measurements, a drop of EMIM-BF<sub>4</sub> was dropped onto the device using a Hamilton Syringe to act as the gate dielectric.

## 3.2 Experimental Setup for SR

Constant drain and source potentials were set through the Keithley 4200SCS using Tungsten probes. The Ionic Liquid was dropped on the P3HT layer so as to completely cover the channel length. A floating platinum electrode was used as the gate electrode. Then, square wave voltage signals were generated using a Keysight 33600A waveform generator. Noise was generated in a different channel of the waveform generator was then superimposed on the signal. This voltage signal with the noise superimposed was then applied at the gate terminal. The current response across the drain-source electrodes was measured versus time. The magnitude Fourier transform of this time series was analysed and Amplitude Spectral Density (ASD) plots were generated using an in-house code that utilised python libraries such as Pandas, Numpy and Matplotlib. The ASD plots gave insights into the frequencies present in the output current.

# Chapter 4

## Results and Findings

### 4.1 Device Characterisation

The layer of P3HT deposited was measured to be about 80nm thick. The channel length was predetermined at 50 microns since pre-patterned ITO coated glass was used as the substrate. The channel width was specified by the radius of the droplet of the Ionic Liquid which was about 900nm. A Keithley 4200-SCS Semiconductor Characterisation System was used for the electrical characterisation of the device. Output characteristics of a transistor consist of the  $I_{DS}$  plotted against the  $V_{DS}$  for varying values of  $V_{GS}$  (see fig4.1).

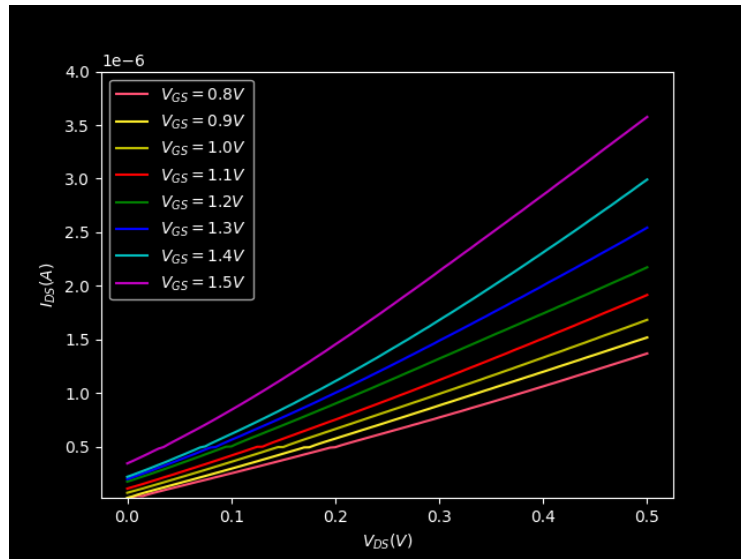


Figure 4.1: The output characteristics of the fabricated device

The transfer characteristics of a FET consist of the  $I_{DS}$  plotted against the  $V_{GS}$  for a fixed value of  $V_{DS}$ . The transfer characteristics were measured and plotted (See fig4.2).

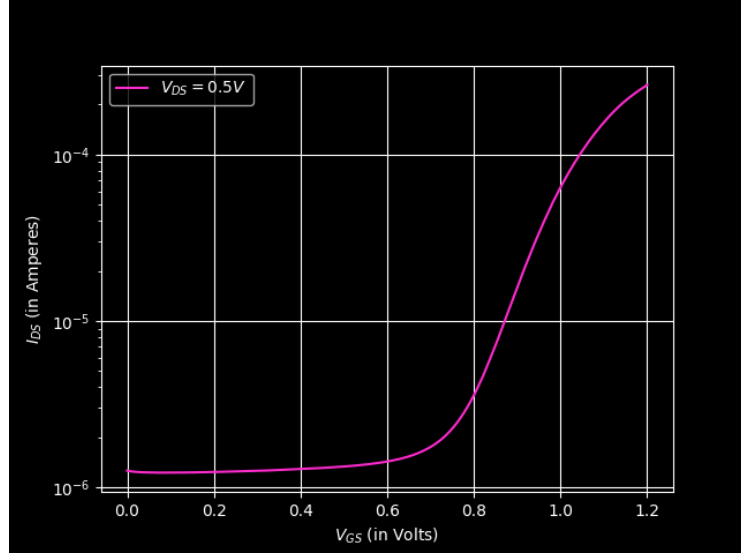


Figure 4.2: The transfer characteristics of the fabricated device

The relationship between  $I_{DS}$  and  $V_{GS}$  for  $V_{GS} > V_{th}$  where  $V_{th}$  is the threshold voltage is given by,

$$I_{DS} = \left( \frac{W\mu C}{2L} \right) (V_{GS} - V_{th})^2 \quad (4.1)$$

where  $W$  and  $L$  are the channel width and length, respectively,  $\mu$  is the charge carrier mobility,  $C$  is the capacitance of the gate dielectric[9]. This relationship can be utilised to find the charge carrier mobility and the threshold voltage by plotting the  $\sqrt{I_{DS}}$  against the  $V_{GS}$  (See fig4.3).

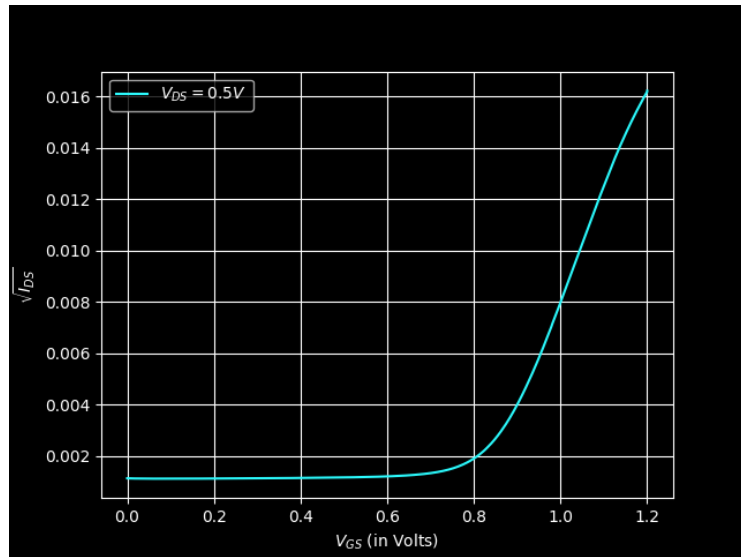


Figure 4.3: The  $\sqrt{I_{DS}}$  vs  $V_{GS}$  plot

The capacitance was found to be  $27\mu F/cm^2$  using an LCR meter. The channel length was pre determined by the pre-patterned ITO coated glass at  $50\mu m$ , the

channel width was determined by the size of the Ionic Liquid dropped. The channel width was found to be  $900\mu m$ . The charge carrier mobility was found using the  $\sqrt{I_{DS}}$  vs  $V_{GS}$  plot to be around  $7.48 cm^2/Vs$ . The threshold voltage was found to be around 850mV.

## 4.2 Stochastic Resonance

The stochastic resonance experiments were carried out using the Keithley 4200SCS. Since the device had a  $V_{th}$  of about 800mV,  $V_{GS} = 1V$  was used as the subthreshold bias whereas  $V_{GS} = 1.4V$  volt was used as the on bias. Using the waveform generator, square waves of amplitude 800mV and frequencies 750mHz, 500mHz and 250mHz were generated (see fig4.4). These were fed as input to the gate terminal in the subthreshold and on state. The  $V_{DS}$  was held constant throughout all the experiments at  $-0.5V$ . The output  $I_{DS}$  was measured as a time series using the Keithley 4200SCS. The sampling mode was set to normal which resulted in a sampling rate of approximately 20Hz giving a Nyquist frequency of 10Hz[16]. This was used to generate the Amplitude Spectral Density (ASD) plots. Once the output for both the on and subthreshold state was recorded, gaussian noise was superimposed on the signal (see fig4.5) and was fed as the input to the gate terminal in the subthreshold state. The current response was once again recorded and analysed.

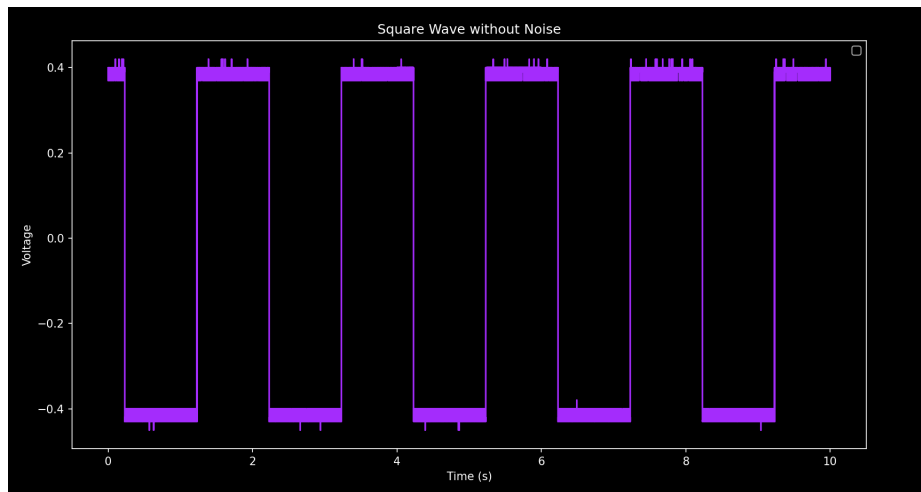


Figure 4.4: The square wave without noise

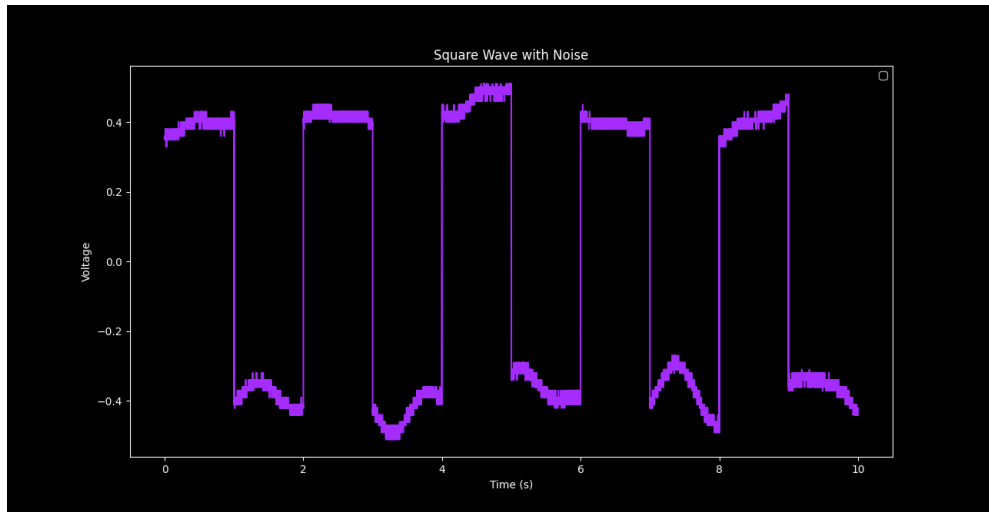


Figure 4.5: The square wave with noise superimposed

### 4.3 Frequency 750mHz

The square wave of 750mHz was applied across the  $V_{GS}$  in the On state, in the Subthreshold state and then in the Subthreshold state with noise superimposed on the square wave. The following results were obtained.

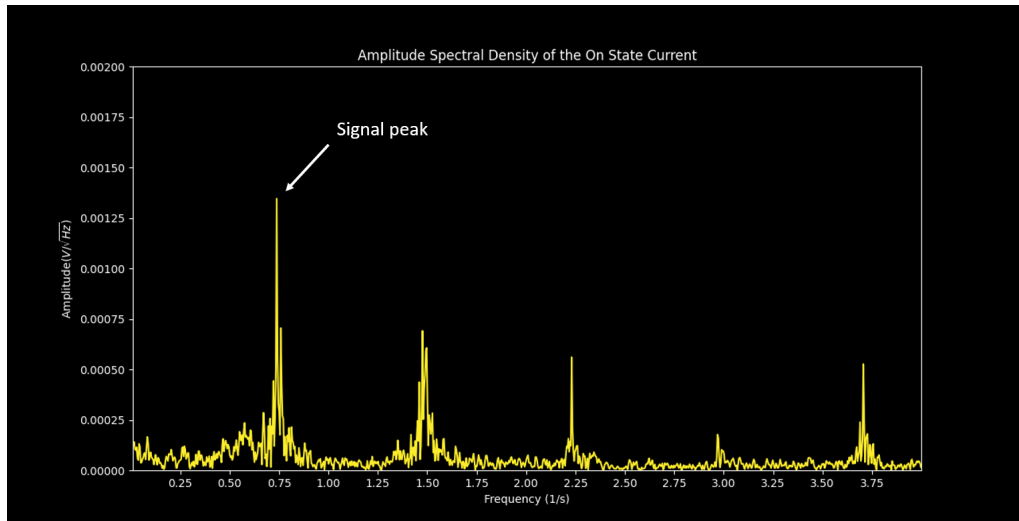


Figure 4.6: The ASD of the On state current.

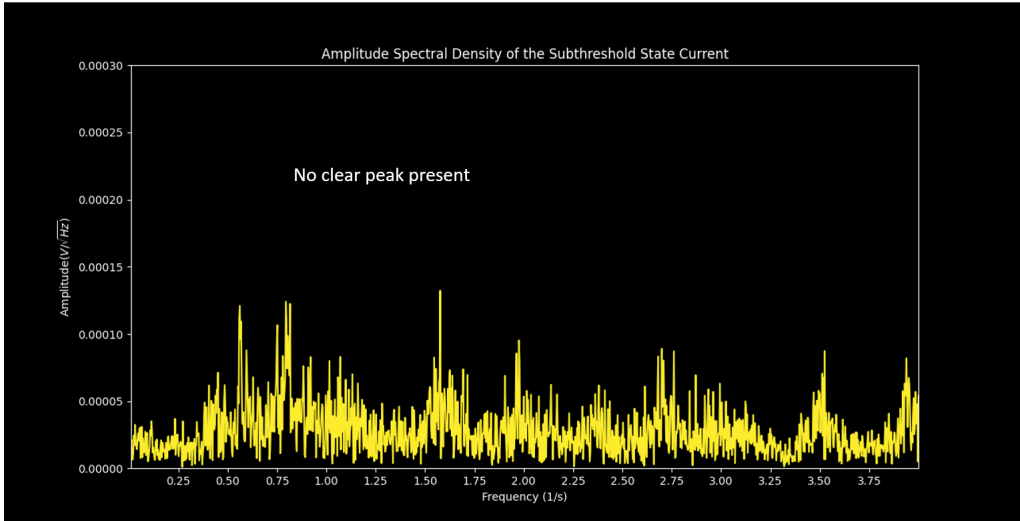


Figure 4.7: The ASD of the Subthreshold state current.

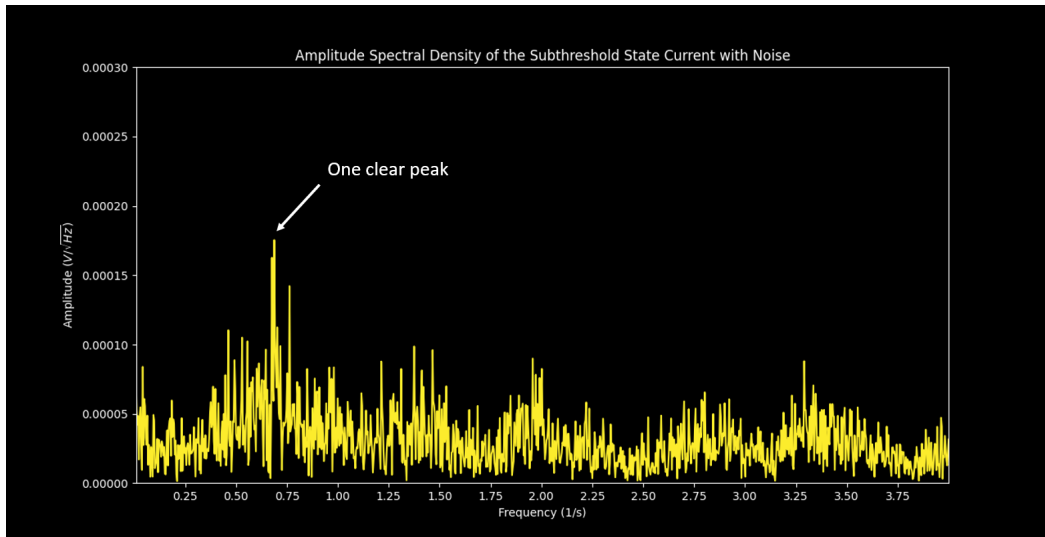


Figure 4.8: The ASD of the Subthreshold state current in the presence of noise.

In the on state, there is a clear peak in the output ASD at the frequency of the input signal, indicating that the signal has been clearly detected (see fig4.6). While there are harmonics of the input signal present at 1.5Hz and 2.25Hz, the peaks are significantly smaller. In the subthreshold state, there are no clear discernible peaks, indicating that the signal has not been picked up by the system (see fig4.7). The ASD of the subthreshold state with the noise however, clearly shows a peak at the frequency of the input frequency (see fig4.8), indicating that the input signal has been detected.

## 4.4 Frequency 500mHz

The square wave of 500mHz was applied across the  $V_{GS}$  in the On state, in the Subthreshold state and then in the Subthreshold state with noise superimposed on the square wave. The following results were obtained.

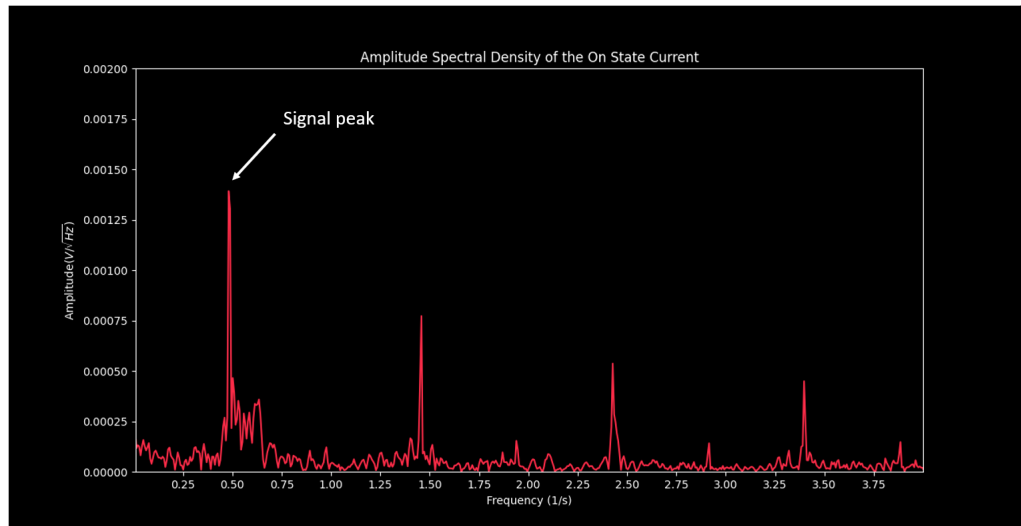


Figure 4.9: The ASD of the On state current.

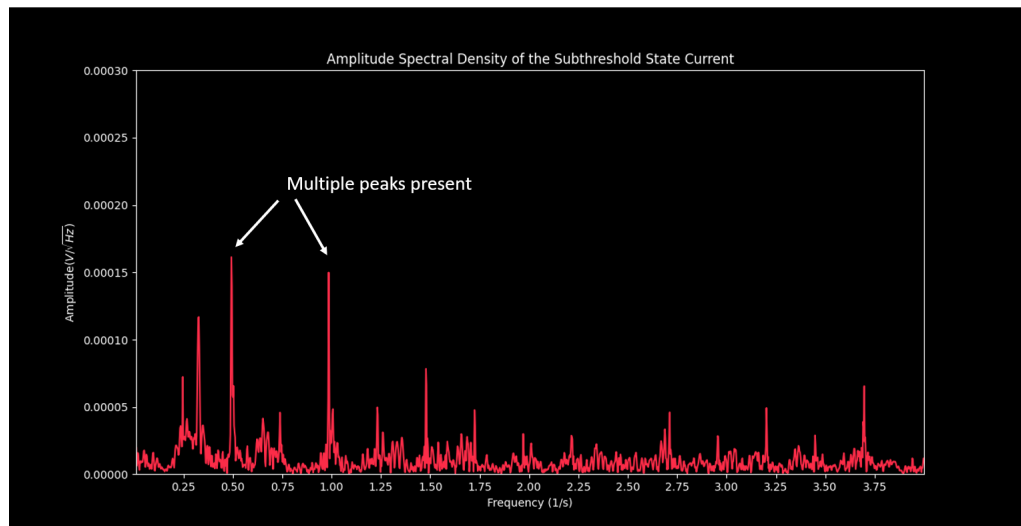


Figure 4.10: The ASD of the Subthreshold state current.

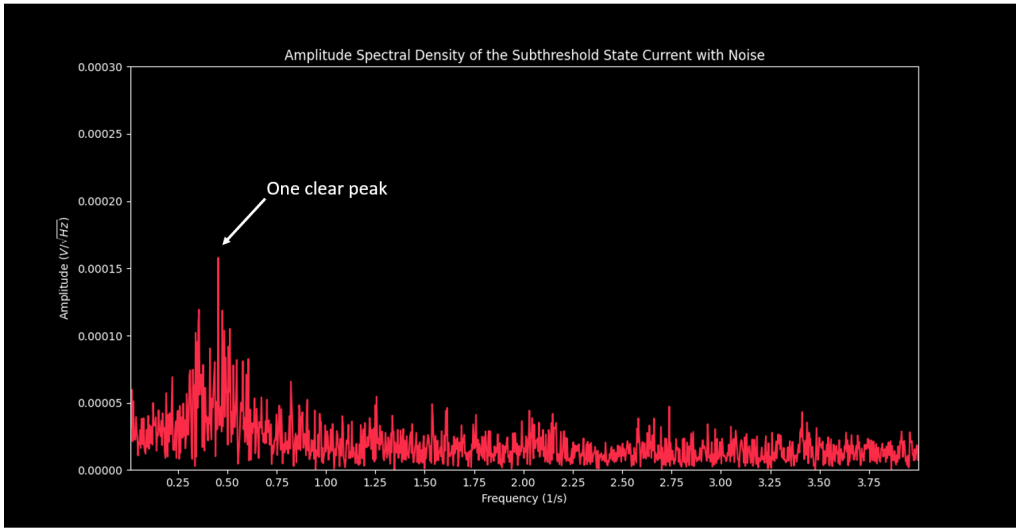


Figure 4.11: The ASD of the Subthreshold state current in the presence of noise.

In the on state, there is a clear peak in the output ASD at the frequency of the input signal, indicating that the signal has been clearly detected (see fig4.9). While there are harmonics of the input signal present at 1.5Hz and 2.5Hz, the peaks are significantly smaller. In the subthreshold state there are multiple peaks present of similar size and it is not possible to discern which belongs to the input signal. (see fig4.10). The ASD of the subthreshold state with the noise however, clearly shows a peak at the frequency of the input frequency (see fig4.11), indicating that the input signal has been detected.

## 4.5 Frequency 250mHz

The square wave of 250mHz was applied across the  $V_{GS}$  in the On state, in the Subthreshold state and then in the Subthreshold state with noise superimposed on the square wave. The following results were obtained.

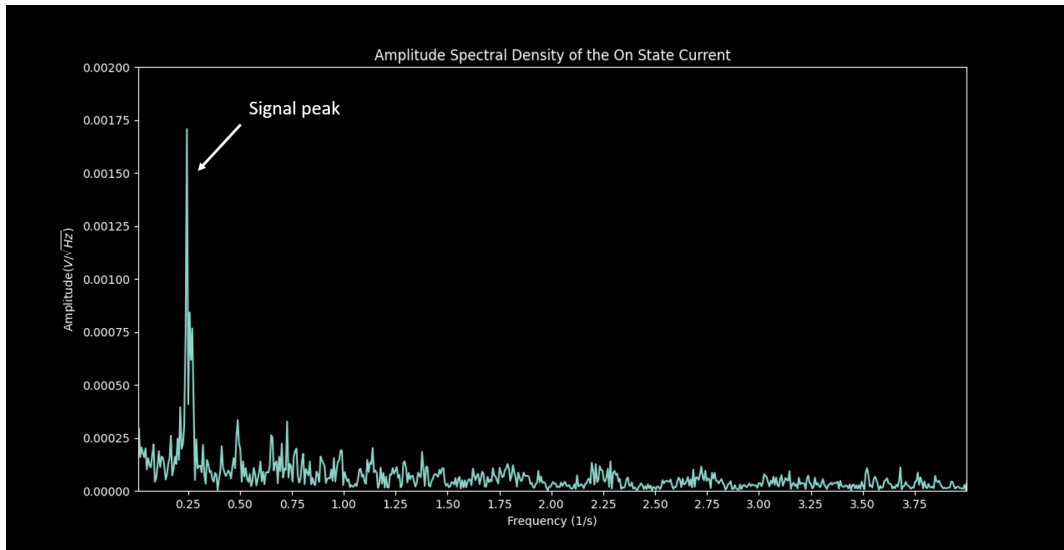


Figure 4.12: The ASD of the On state current.

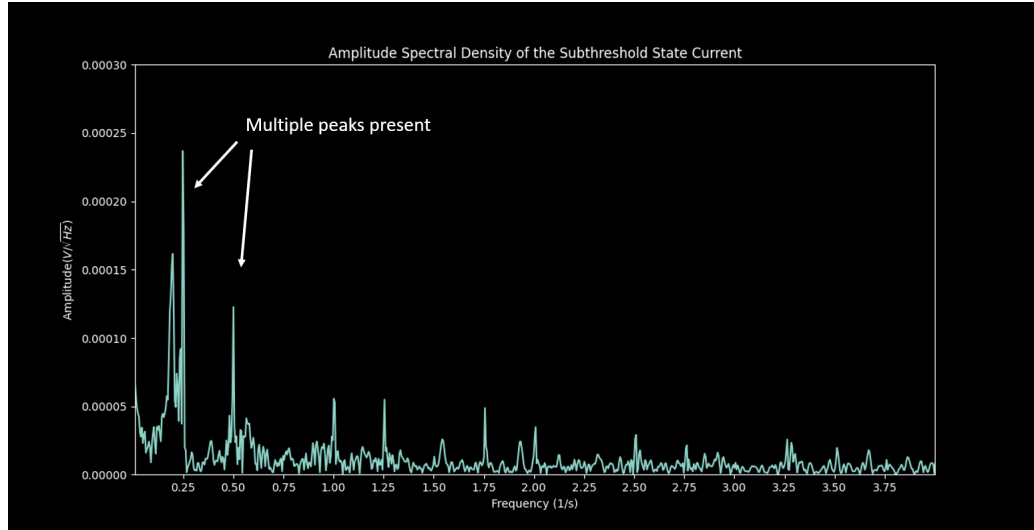


Figure 4.13: The ASD of the Off state current.

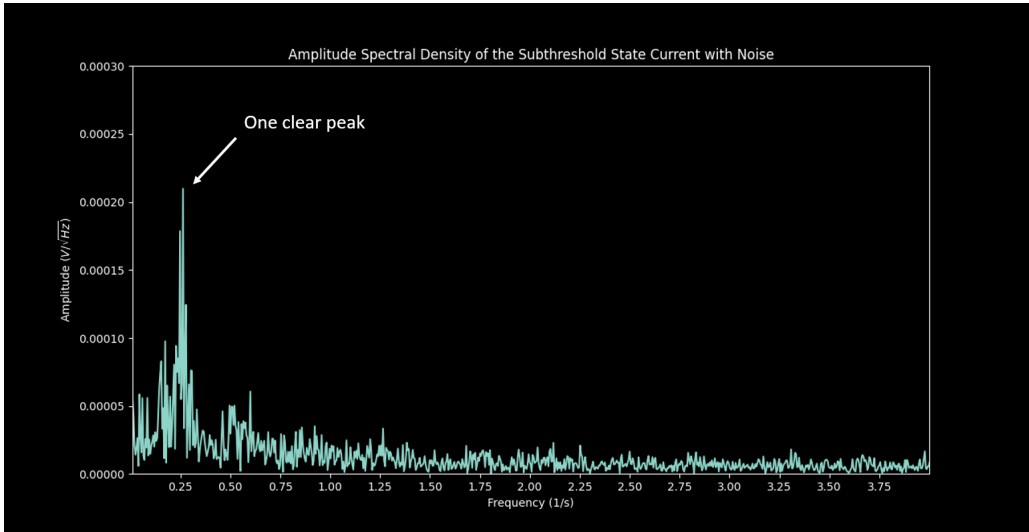


Figure 4.14: The ASD of the Subthreshold state current in the presence of noise.

In the on state, there is a clear peak in the output ASD at the frequency of the input signal and no other peaks are present, indicating that the signal has been clearly detected (see fig4.12). In the subthreshold state there are multiple peaks present and hence, one cannot be sure of the frequency of the input signal. (see fig4.13). The ASD of the subthreshold state with the noise however, clearly shows a peak at the frequency of the input frequency (see fig4.14), indicating that the input signal has been detected.

# **Chapter 5**

## **Conclusions**

### **5.1 Conclusions**

In this project, an ionic liquid gated organic field effect transistor was successfully fabricated. The electrical characterisation of the device was successfully carried out. Due to the electric-double layer formation, very high capacitance and charge carrier mobility values were achieved. In order to demonstrate stochastic resonance, square voltage signals of three different frequencies were generated and used as input signals at the gate terminal in the On and subthreshold states. A clear improvement in the device's ability to detect signals in the subthreshold state was observed in the presence of external noise.

### **5.2 Scope for future work**

While the concept of using noise to amplify signals was successfully demonstrated, quite a few challenges need to be solved in order to utilise this concept in practice. It may be possible in the future to collect data on the type of background noise present in the application environment of a device, and then tune materials used in fabrication to utilise the background noise to enhance the performance of the device. Ionic liquid gated device have slow response times and are unable to operate at high frequencies. New techniques/device structures may help in tackling this problem.

# Bibliography

- [1] *1956 Nobel prize in physics*. URL: <https://www.bell-labs.com/about/awards/1956-nobel-prize-physics/#gref>.
- [2] World Population Review. URL: <https://worldpopulationreview.com/country-rankings/semiconductor-manufacturing-by-country>.
- [3] Wikipedia contributors. *List of countries by silicon production* — Wikipedia, The Free Encyclopedia. [Online; accessed 2-May-2023]. 2022. URL: [https://en.wikipedia.org/w/index.php?title=List\\_of\\_countries\\_by\\_silicon\\_production&oldid=1122448377](https://en.wikipedia.org/w/index.php?title=List_of_countries_by_silicon_production&oldid=1122448377).
- [4] Yoshiharu Suzuki and Naoki Asakawa. “Stochastic Resonance in Organic Electronic Devices”. In: *Polymers* 14.4 (2022), p. 747.
- [5] John K Douglass et al. “Noise enhancement of information transfer in crayfish mechanoreceptors by stochastic resonance”. In: *Nature* 365.6444 (1993), pp. 337–340.
- [6] Fabio Ciciora and Clara Santato. “Organic light emitting field effect transistors: advances and perspectives”. In: *Advanced Functional Materials* 17.17 (2007), pp. 3421–3434.
- [7] Takuya Fujimoto and Kunio Awaga. “Electric-double-layer field-effect transistors with ionic liquids”. In: *Physical Chemistry Chemical Physics* 15.23 (2013), pp. 8983–9006.
- [8] Akhil Doddla et al. “Stochastic resonance in MoS<sub>2</sub> photodetector”. In: *Nature communications* 11.1 (2020), p. 4406.
- [9] D. Neamen. *Semiconductor Physics And Devices*. McGraw-Hill Higher Education, 2011. ISBN: 9780077418847. URL: [https://books.google.co.in/books?id=R%5C\\_xKAgAAQBAJ](https://books.google.co.in/books?id=R%5C_xKAgAAQBAJ).
- [10] M Singh et al. “The double layer capacitance of ionic liquids for electrolyte gating of ZnO thin film transistors and effect of gate electrodes”. In: *Journal of Materials Chemistry C* 5.14 (2017), pp. 3509–3518.

- [11] *Ito glass substrates, 20 x 15 mm, Ofet and sensing.* URL: <https://www.ossila.com/en-in/products/interdigitated-ito-ofet-substrates>.
- [12] Zhenan Bao, Ananth Dodabalapur, and Andrew J Lovinger. “Soluble and processable regioregular poly (3-hexylthiophene) for thin film field-effect transistor applications with high mobility”. In: *Applied physics letters* 69.26 (1996), pp. 4108–4110.
- [13] Yogesh Yadav, Sajal Kumar Ghosh, and Samarendra Pratap Singh. “High-performance organic field-effect transistors gated by imidazolium-based ionic liquids”. In: *ACS Applied Electronic Materials* (2021).
- [14] Merck. *Poly(3-decylthiophene-2,5-diyl)*. [Online; accessed 3-May-2023]. 2023. URL: <https://www.sigmaaldrich.com/IN/en/product/aldrich/495344?context=product>.
- [15] Thermo Fisher Scientific. *L19763 1-Ethyl-3-methylimidazolium tetrafluoroborate*. [Online; accessed 3-May-2023]. 2023. URL: <https://www.alfa.com/en/catalog/L19763/>.
- [16] Wikipedia contributors. *Nyquist frequency — Wikipedia, The Free Encyclopedia*. [Online; accessed 3-May-2023]. 2023. URL: [https://en.wikipedia.org/w/index.php?title=Nyquist\\_frequency&oldid=1145284140](https://en.wikipedia.org/w/index.php?title=Nyquist_frequency&oldid=1145284140).